Biochimica et Biophysica Acta 1833 (2013) 2734–2744

Contents lists available at ScienceDirect

Biochimica et Biophysica Acta

journal homepage: www.elsevier.com/locate/bbamcr

The small GTPase N-Ras regulates extracellular matrix synthesis, proliferation and migration in fibroblasts

Isabel Fuentes-Calvo [a,b], Piero Crespo [c], Eugenio Santos [d], José M. López-Novoa [a,b], Carlos Martínez-Salgado [a,b,e,*]

[a] Unidad de Fisiopatología Renal y Cardiovascular, Instituto "Reina Sofía" de Investigación Nefrológica, Departamento de Fisiología y Farmacología, Universidad de Salamanca, Salamanca, Spain
[b] Instituto de Investigación Biomédica de Salamanca (IBSAL), Salamanca, Spain
[c] Instituto de Biomedicina y Biotecnología de Cantabria (IBBTEC), Consejo Superior de Investigaciones Científicas (CSIC), IDICAN, Universidad de Cantabria, Cantabria, Spain
[d] Centro de Investigación del Cáncer, Universidad de Salamanca, Consejo Superior de Investigaciones Científicas (CSIC), Salamanca, Spain
[e] Instituto de Estudios de Ciencias de la Salud de Castilla y León (IECSCYL), Unidad de Investigación, Hospital Universitario de Salamanca, Salamanca, Spain

ARTICLE INFO

Article history:
Received 19 September 2012
Received in revised form 9 July 2013
Accepted 10 July 2013
Available online 18 July 2013

Keywords:
Ras proteins
PI3K/Akt
MEK/ERK 1/2
Transforming growth factor-β1
Renal fibrosis

ABSTRACT

In addition to their role as oncogenes, Ras GTPases are key regulators of cell function. There is a proven relationship between the signaling pathways of transforming growth factor-β1 (TGF- β1) and Ras GTPases. Each of the Ras isoforms (H, N and K) exhibits specific modulatory activity on different cellular pathways. Our purpose has been to study some of the mechanisms involved in the development of renal fibrosis, assessing the individual role of N-Ras in basal and TGF-β1-mediated extracellular matrix (ECM) synthesis, proliferation, and migration in immortalized N-Ras deficient fibroblasts (N-*ras*$^{-/-}$). Compared to normal counterparts, fibroblasts deficient for N-Ras exhibited higher basal activity levels of phosphatidylinositol-3-kinase (PI3K)/Akt and MEK/Erk, accompanied by upregulated collagen synthesis and diminished proliferation and migration rates. We found that the absence of N-Ras did not affect TGF-β1-induced proliferation and migration, which required PI3K/Akt but not Erk1/2 activation. Similar effector pathway dependence was found for fibronectin and collagen type I expression. Our results indicate that N-Ras might contribute to renal fibrosis through the down-regulation of ECM synthesis and up-regulation proliferation and migration modulating Akt activation. N-Ras also regulates TGF-β1-induced collagen I and fibronectin expression through Erk-independent pathways.

1. Introduction

Ras superfamily encompasses more than 150 small GTPases, divided into at least 5 distinct subfamilies (Ras, Rho/Rac, Rab, Arf, and Ran). The mammalian Ras subfamily, initially described as pro-oncogenes, includes three *ras* genes and four 21 kDa proteins highly conserved across different species: H-Ras, N-Ras, K-Ras4A and K-Ras4B that play functionally significant roles in numerous cellular processes, including proliferation, survival and differentiation [1–5]. These Ras proteins are ubiquitously expressed in all cell lineages and organs, although there are quantitative and qualitative differences in expression through tissues or development stage [6,7]. In addition, specific intracellular processing and localization in different membrane microdomains or subcellular compartments of each Ras isoform may provide further biological basis for isoform specific function [6,8–14].

Ras cycles between an inactive GDP-bound form and an active GTP-bound form. Activated Ras isoforms may interact with several effector pathways, including phosphatidylinositol 3-kinase-protein kinase B (PI3K-Akt) and MEK/Erk1/2 [15]. Activation of MEK/Erk pathway controls cell-cycle progression, differentiation and apoptosis [16] while PI3K/Akt pathway is implicated in regulation of cell metabolism, proliferation, cell motility and promotion of cell survival protecting cells from apoptosis [17].

Transforming growth factor-β (TGF-β), a cytokine involved in extracellular matrix (ECM) homeostasis and control of cell proliferation [18–23], and Ras signaling pathways have numerous relationships. For example, during epithelial regeneration TGF-β antagonizes mitogenic Ras signaling, but in tumor progression TGF-β and Ras act synergistically [24]. Ras GTPases participate downstream in the signaling of TGF-β, and share some signal pathways such as PI3K/Akt and MEK/Erk 1/2 [25–29]. Fibroblast proliferation and migration play a major role in the genesis of renal fibrosis [30] and this can be extended to other models of fibrosis [31]. There are studies suggesting different functional roles for each Ras isoform in proliferation, migration and ECM expression [32–34]. Previous studies of our group have shown that the lack of both H- and N-Ras isoforms in fibroblasts is associated to increased ECM synthesis and reduced fibroblast proliferation [33]. Recently we have also demonstrated that the H-Ras isoform down-regulates ECM synthesis and stimulates

Abbreviations: TGF-β1, transforming growth factor-β1; ECM, extracellular matrix; PI3K-Akt, phosphatidyl inositol 3 kinase-protein kinase B; MEK-Erk1/2, mitogen activated protein kinase 2-extracellular signal regulated kinase 1/2

* Corresponding author at: Unidad de Investigación, Hospital Universitario de Salamanca, Paseo San Vicente 58-182, 37007 Salamanca, Spain. Tel.: +34 923 294500x1945; fax: +34 923 294669.
E-mail address: carlosms@usal.es (C. Martínez-Salgado).

0167-4889/$ – see front matter © 2013 Elsevier B.V. All rights reserved.
http://dx.doi.org/10.1016/j.bbamcr.2013.07.008

proliferation and migration by modulating PI3K/Akt and MEK/Erk activation in fibroblasts [32]. In agreement with these results, in an in vivo model of obstructive nephropathy in mice we have reported that H-Ras regulates tubule-interstitial fibrosis and myofibroblasts proliferation [35]. However, to date there are no studies analyzing the role of the N-Ras isoform in the processes that trigger and regulate renal fibrosis. For this reason, the purpose of the present study has been to assess the effect of N-Ras deficiency in basal and TGF-β1-mediated ECM synthesis, proliferation and migration in cultured embryonic fibroblasts isolated from mice lacking the N-Ras isoform (N-*ras*$^{-/-}$). The Ras signaling pathways MEK/Erk and PI3K/Akt have also been studied to elucidate their possible role in ECM synthesis, proliferation and migration in the absence of N-Ras.

2. Materials and methods

2.1. Materials and reagents

Crystal violet was from Fluka (Buchs, Switzerland). Rabbit anti-mouse Akt 1/2 and rabbit anti-rat Erk1, and mouse anti-human phospho-Erk antibodies were from Santa Cruz Biotechnology (Santa Cruz, CA., USA.). Rabbit anti-human phospho-Akt antibody was from Cell Signalling Technology (Danvers, MA USA). Rabbit anti-mouse collagen type I and fibronectin antibodies, PVDF membrane, Ras GTPase Elisa Kit and magnesium lysis buffer (MLB) were from Upstate Biotechnology (Waltham, MA, USA). Mouse anti-human PCNA antibody was from BD-Transduction Laboratories (San Jose, CA, USA). Rabbit anti-human Ki67 was obtained from MD (Granada, Spain). Goat anti-rabbit Cy3 was from Jackson Immunoresearch (West Grove, PA, USA). Goat anti-rabbit and anti-mouse IgG (H + L) horseradish peroxidase (HRP) conjugated antibodies and Dc protein assay were from BioRad (Hercules, CA, USA). Hoechst 33258 was from Molecular Probes (Barcelona, Spain). ECL chemiluminescence Western blotting system and Hyperfilm X-ray film were from GE-Healthcare (Chalfont St. Giles, United Kingdom). Tri-reagent was from Molecular Research Center (Cincinnati, OH, USA). JetPEI transfection reagent was from Polyplus Transfection (Illkirch, France). TGF-β1 was from R&D Systems (Minneapolis, MN, USA). U0126 and LY294002 were from Calbiochem-Merk (Madrid, Spain). [^{3}H] proline was from American Radiolabelled Chemical (St. Louis, MO, USA). Fetal calf serum (FCS), Dulbecco's modified Eagle's medium (DMEM) and trypsin solution were from Gibco-Invitrogen (Grand Island, NY, USA). The sterile plastic material used in cell culture was from Nunc (Roskilde, Denmark). Cell culture inserts were from Falcon (Madrid, Spain). Wallac 1409 DSA liquid scintillation counter was from Perkin Elmer (Waltham, MA, USA) and Scion Image software was from Scion Corporation (Frederick, MD, USA). All other reagents were of analytical grade and obtained from Sigma Química (Madrid, Spain), and Merck (Madrid, Spain).

2.2. Cell culture and growth factor stimulation

WT and N-*ras*$^{-/-}$ mouse embryonic fibroblasts were subcultured and immortalized as previously reported [36]. Briefly, N-Ras KO fibroblasts (N-*ras*$^{-/-}$) were cultured from N-*ras*$^{-/-}$ mouse embryos which were recovered at day post coitum 15–17 and were treated with trypsin-ethylenediaminetetraacetic acid (EDTA) 0.25% (Gibco-BRL, Cheshire, UK) for 30 min before plating. Immortalized cultures that survived crisis after 15–20 passages were identified and cloned and their genotypes reconfirmed by PCR analysis as previously reported [36].

Immortalized cells were grown in DMEM medium containing 10% FCS and 100 U/mL penicillin/streptomycin at 37 °C, 5% CO_2. For Western blot and PCR analysis cells were seeded in 100 mm Petri dishes, for total collagen measurements and proliferation studies cells were plated at 20,000 or 9000 cells/well in 24 well plates, respectively. When cultures achieved 80–90% confluence, cells were serum-starved for 24 h and treated with active human recombinant TGF-β1 (1 ng/mL) or control vehicle during 24 h in the absence of serum. When pharmacological inhibition was used, mitogen activated kinase/Erk kinase-1 (MEK-1) inhibitor U0126 (20 μM) or the PI3K inhibitor LY294002 (20 μM) were added 30 min before TGF-β1 stimulation.

2.3. Crystal violet staining

Total cell number was measured using a colorimetric method previously described [37]. Briefly, cells in 24 well plates were fixed for 10 min with 10% glutaraldehyde, stained in 1% crystal violet solution for

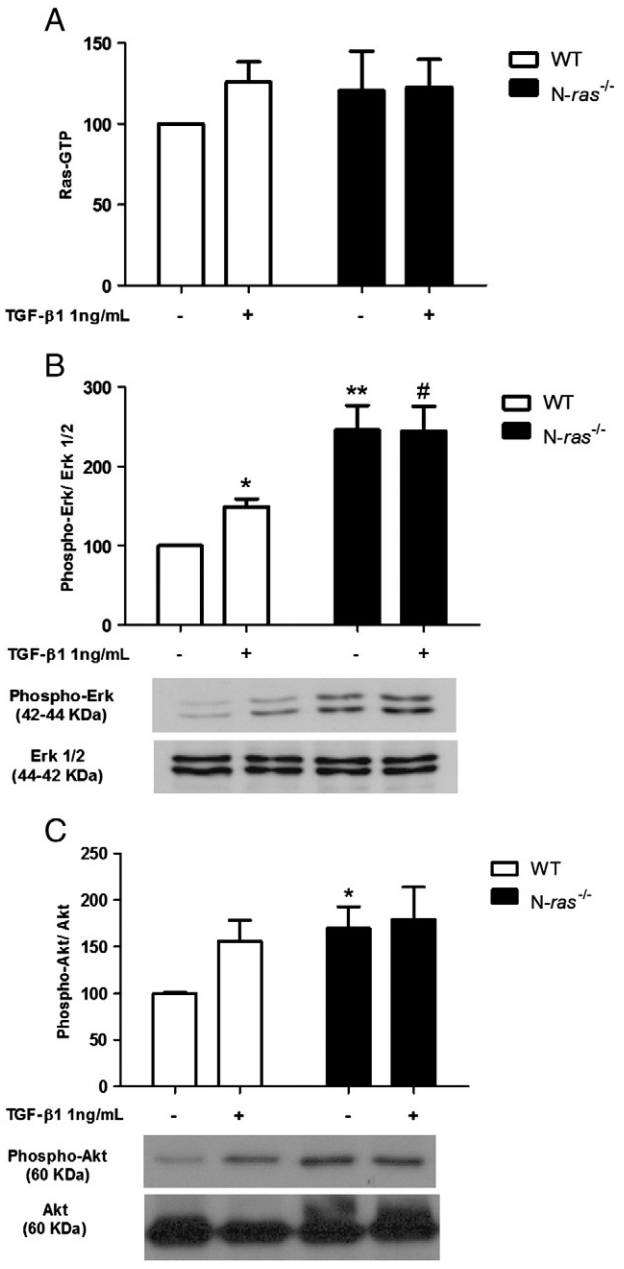

Fig. 1. Ras activation and expression of Ras effectors, Erk and Akt in WT and N-*ras*$^{-/-}$ fibroblasts. Ras-GTP evaluated by ELISA (A); phospho-Erk (B) and phospho-Akt (C) protein expressions evaluated by Western blot. Histograms in (A) represent the mean ± standard error of the mean (SEM) of the luminescence of 3 experiments measured by triplicate, expressed as percentage over basal values (WT fibroblasts in 0.5% FCS, 100%). Histograms in B and C represent the mean ± SEM of the optical density of the bands, expressed as percentage over basal values (WT fibroblasts in 0.5% FCS, 100%). Histograms correspond to the ratio phospho-Erk 1/2/Erk 1/2 or phospho-Akt/Akt expression. Lower panel in B–C shows a representative blot of 42 (WT)-17 (N-*ras*$^{-/-}$) experiments, performed under similar conditions. Statistically significant differences: *($p < 0.05$) or **($p < 0.01$) vs. WT fibroblasts in basal conditions; #($p < 0.01$) vs. WT fibroblasts treated with 1 ng/mL TGF-β1.

30 min, dried overnight, dissolved with 10% acetic acid and optical absorbance was measured at 595 nm, which was proportional to the number of viable cells in each well.

2.4. Immunofluorescence analysis of Ki67 expression

Nuclear Ki-67 staining indicates the proliferating cells [38]. Cells on cover slips were fixed with 4% paraformaldehyde, washed with phosphate buffer saline (PBS: 0.81% NaCl, 2.6 mM H_2KPO_4, 4.1 mM HNa_2PO_4), permeabilized with 0.1% Triton X-100, blocked 30 min with 2% BSA in PBS, treated with PBS-0.05% Tween-20 for 10 min, incubated for 2 h with rabbit anti-human Ki67 (dilution 1/50) in PBS, and incubated for 30 min with goat anti-rabbit Cy3 (1/1000) in PBS in a dark chamber. Nuclei staining were performed by 5 min incubation with 3 μM Hoechst 33258 in the dark. Confocal images were obtained using a Zeiss Axiovert 200M microscope with a HeNe laser with 543-excitation

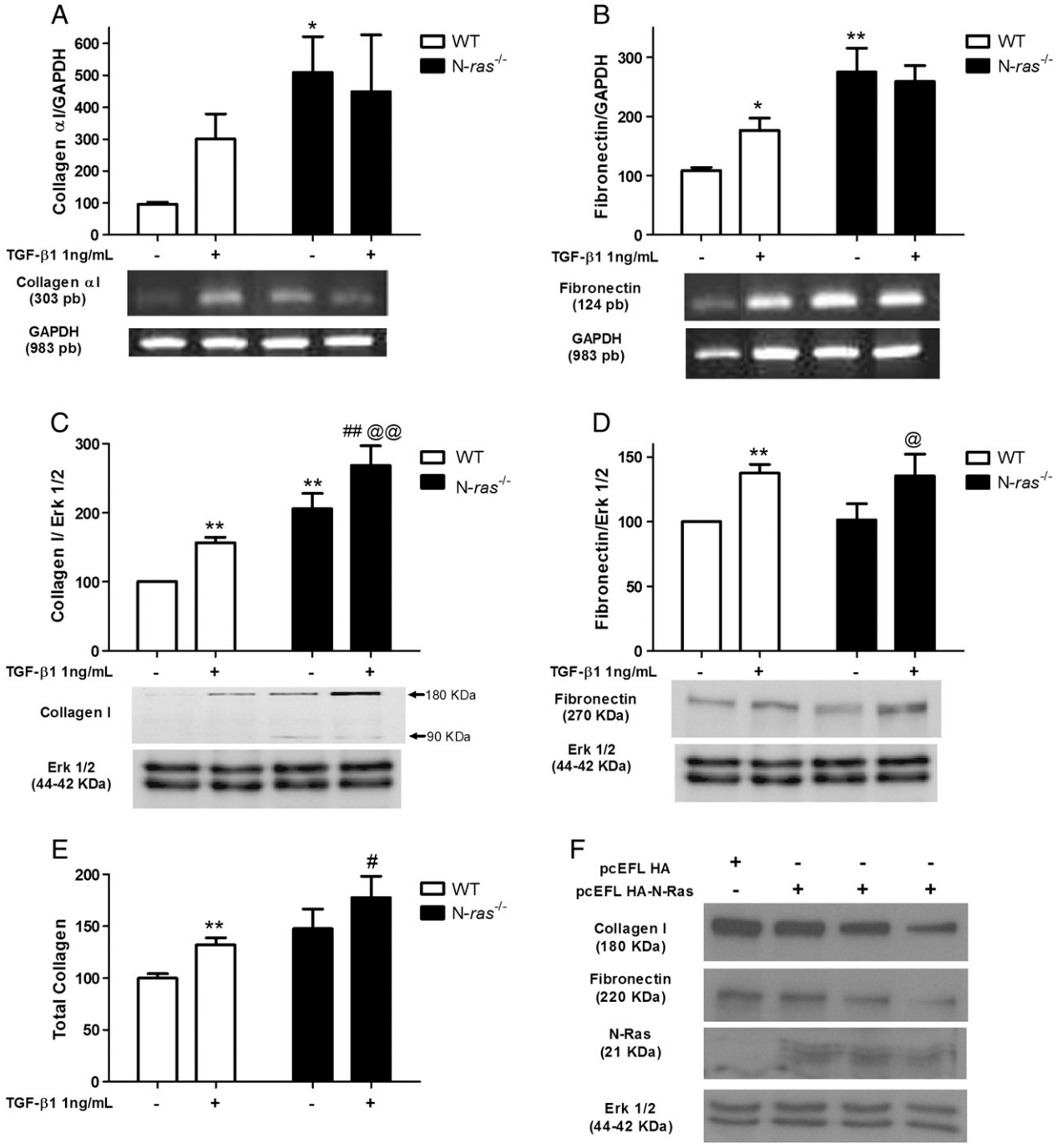

Fig. 2. Expression of ECM proteins in WT and N-*ras*$^{-/-}$ fibroblasts. Collagen type α1 (A) and fibronectin (B) mRNA expression evaluated by RT-PCR; collagen type I (C) and fibronectin (D) protein expression evaluated by Western blot; total collagen synthesis (E) evaluated by [^{3}H] proline incorporation; effect of N-Ras re-introduction on collagen type I and fibronectin expression in N-*ras*$^{-/-}$ fibroblasts (F). Lower panels in A and B show a representative picture of 4 (WT)–6 (N-*ras*$^{-/-}$) different RT-PCR experiments. Lower panels in C and D show a representative blot of 6 (N-*ras*$^{-/-}$)–42 (WT) experiments, performed under similar conditions. Histograms in A–D represent the mean ± SEM of the optical density of the bands, expressed as percentage over basal values (WT fibroblasts in 0.5% FCS, 100%), and correspond to the ratio fibronectin or collagen/Erk 1/2 expression or GAPDH (used as loading control). Histograms in E represent the mean ± SEM of 16 (N-*ras*$^{-/-}$)-42 (WT) experiments expressed as percentage over basal values (WT fibroblasts in 0.5% FCS, 100%), performed in triplicate. Statistically significant differences: *($p < 0.05$) or **($p < 0.01$) vs. WT fibroblasts in basal conditions; #($p < 0.01$) or ##($p < 0.05$) vs. WT fibroblasts treated with 1 ng/mL TGF-β1; @($p < 0.05$) or @@($p < 0.01$) vs. N-*ras*$^{-/-}$ fibroblasts in basal conditions.

for rhodamine and Hg laser with 365-excitation for DAPI. All captured images had identical parameters for intensity, pinhole aperture, etc.

2.5. Ras activation

Ras-GTP in total cell lysates (50 μg) was quantified by the Ras activation ELISA assay Kit following the manufacturer's instructions. Ras GTP activation is expressed in n-fold vs. control.

2.6. Western blot analysis

Western blot was performed as previously described [33]. Membranes were incubated with the following antibodies: anti-Akt 1/2 (dilution: 1/1000), anti-Erk1 (1/10,000), anti-phospho-Erk (1/2000), anti-phospho-Akt (1/1000), anti collagen type I (1/20,000), anti-fibronectin (1/30,000), anti-PCNA (1/5000) and anti-Ras (1/1000). We used total Erk 1/2 levels as controls for protein loading because their basal levels showed no differences between WT and N-*ras*$^{-/-}$ fibroblasts after TGF-β1 treatment, as we had previously found in H-Ras KO and H- and N-Ras double KO fibroblasts [32,33], whereas other proteins frequently used as loading controls (actin, tubulin) were affected after TGF-β1 treatment.

2.7. Polymerase chain reaction

PCR was performed as previously described [33]. Primers: for mouse fibronectin, bp 79 to 99, 5′-ATG TGG ACC CCT CCT GAT AGT-3′, and bp 182 to bp 202, 5′-GCC CAG TGA TTT CAG CAA AGG-3′. For human collagen type I (α1), bp 5292 to 3314, 5′-TGT TGC TGA AAG ACT ACC TCG T-3′, and bp 5572 to 5594, 5′-CCT CCC ATG TTA AAT AGC ACC T-3′.

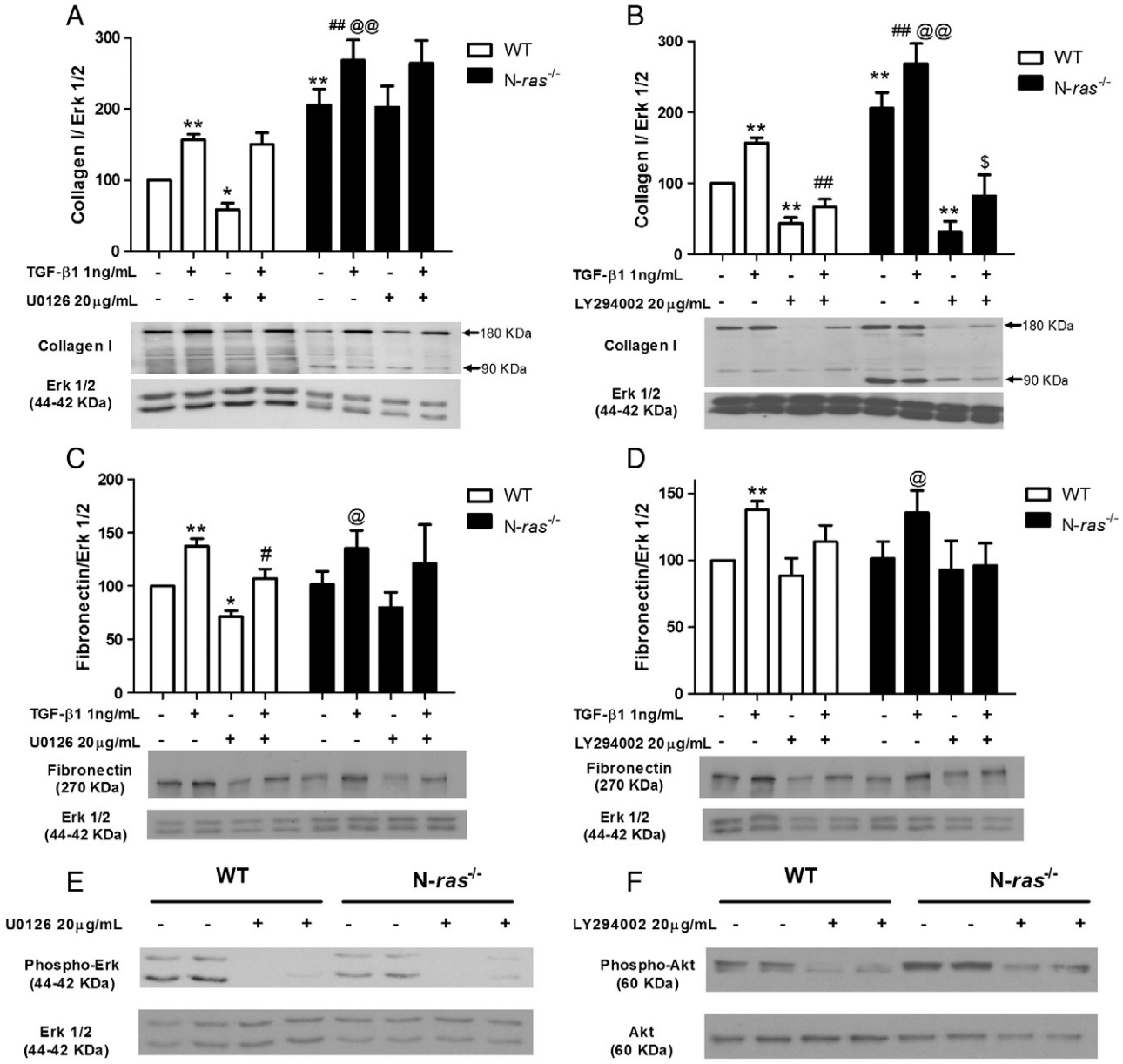

Fig. 3. Effect of MEK/Erk1/2 and PI3K/Akt inhibition on the expression of ECM proteins in WT and N-*ras*$^{-/-}$ fibroblasts. Effect of phospho-Erk inhibition with 20 μM U0126 on collagen type I (A), fibronectin (C) and phospho-Erk (E) protein expression evaluated by Western blot; and effect of phospho-Akt inhibition with 20 μM LY294402 on collagen type I (B), fibronectin (D) and phospho-Akt (F) protein expression evaluated by Western blot. Lower panels in A–D show a representative blot of 6 (N-*ras*$^{-/-}$)-42 (WT) experiments, performed under similar conditions. A–D histograms represent the mean ± SEM of the optical density of the bands, expressed as percentage over basal values (WT fibroblasts in 0.5% FCS, 100%); histograms correspond to the ratio fibronectin or collagen/Erk 1/2. Statistically significant differences: *($p < 0.05$) or **($p < 0.01$) vs. WT fibroblasts in basal conditions; #($p < 0.01$) or ##($p < 0.05$) vs. WT fibroblasts treated with 1 ng/mL TGF-β1; @($p < 0.05$) or @@($p < 0.01$) vs. N-*ras*$^{-/-}$ fibroblasts in basal conditions; $($p < 0.01$) vs. N-*ras*$^{-/-}$ fibroblasts treated with 1 ng/mL TGF-β1.

For GAPDH, 5′-TGA AGG TCG GTG TGA ACG GAT TTG GC-3′ and 5′-CAT GTA GGC CAT GAG GTC CAC CAC-3′. Cycling conditions for collagen I: 95 °C, 5 min, 40 cycles of 1 min 95 °C, 1 min 52 °C and 1 min 72 °C, and an elongation cycle of 5 min 72 °C; for fibronectin: 5 min 95 °C, 35 cycles of 1 min 95 °C, 1 min 61.6 °C, and 1 min 72 °C, and an elongation cycle of 5 min 72 °C; for GAPDH: 5 min 94 °C, 28 cycles of 1 min 94 °C, 1 min 60 °C, and 1.5 min 72 °C, and an elongation cycle of 5 min 72 °C, using a Bio-Rad Thermal Cycler. Amplified products were analyzed by electrophoresis in 1.5% agarose gels.

2.8. Total collagen synthesis measurement

The incorporation of [^{3}H]-proline into collagen proteins was used to quantify collagen content in the culture medium, as described elsewhere [39]. Radiolabeling was performed incubating 0.15 mM β-aminopropionitrile, 210 mM ascorbic acid, 183 mM proline and 1 μCi/well [^{3}H]-Proline (specific activity: 40 Ci/mmol) for 24 h in fresh DMEM serum-free medium. Proteins were precipitated in ice-cold 10% trichloroacetic acid and the pellet was washed and resuspended in

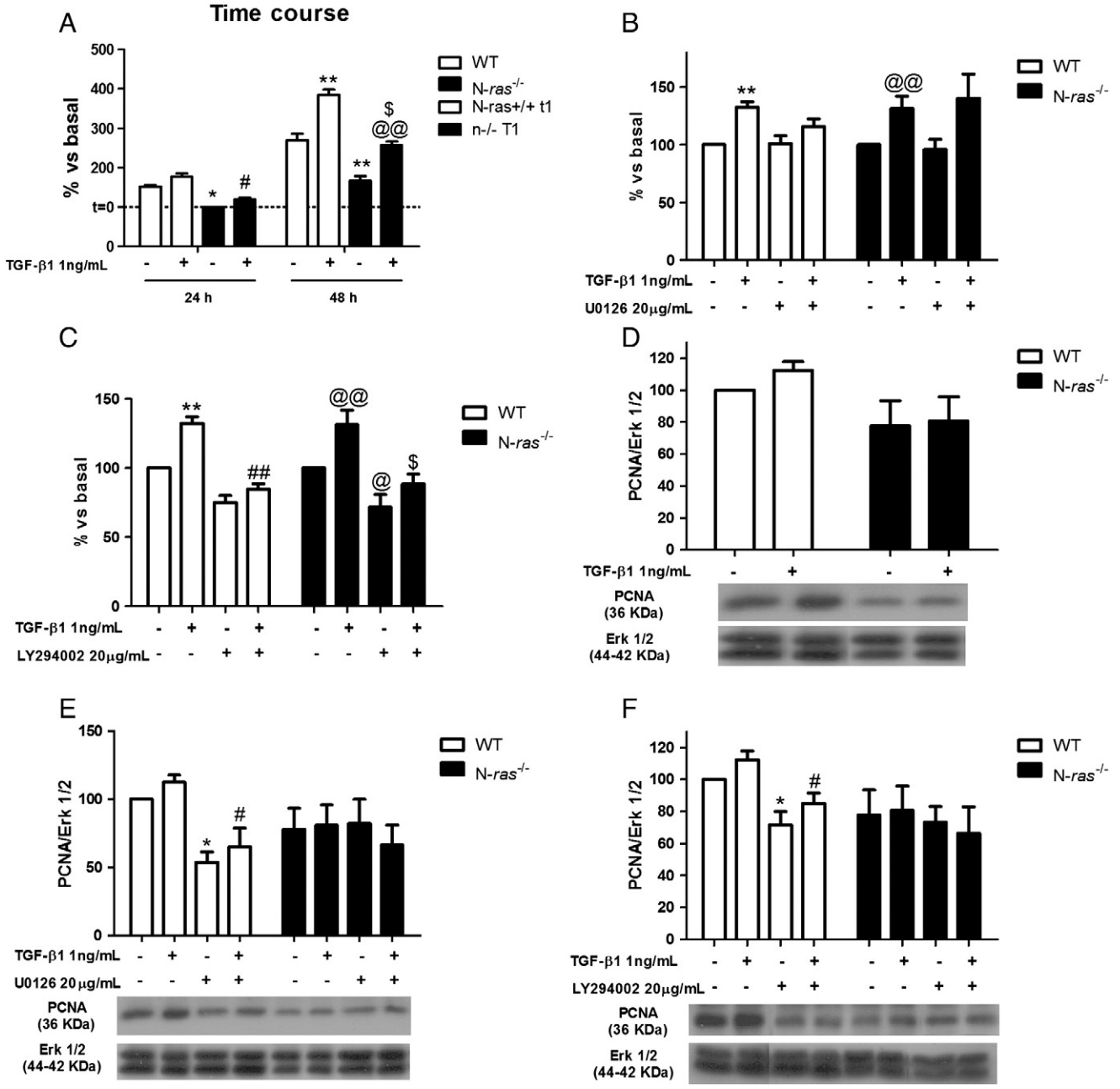

Fig. 4. WT and N-*ras*$^{-/-}$ fibroblast proliferation and PCNA expression. Effect of TGF-β1 treatment (1 ng/mL) on fibroblasts proliferation measured at 24–48 h by crystal violet staining (A); phospho-Erk inhibition with 20 μM U0126 (B) and phospho-Akt inhibition with 20 μM LY294002 (C) on fibroblasts proliferation evaluated by crystal violet staining; effect of TGF-β1 treatment (1 ng/mL) (D), phospho-Erk inhibition with 20 μM U0126 (E) and phospho-Akt inhibition with 20 μM LY294002 (F) on PCNA protein expression evaluated by Western blot. Histograms in A–C represent the mean ± SEM of 8–32 (WT) and 8 (N-*ras*$^{-/-}$) experiments, performed in triplicate and expressed as percentage over basal values (WT and N-*ras*$^{-/-}$ fibroblasts in 0.5% FCS, 100%). Lower panels in D–E show representative blots of 32 (WT)–8 (N-*ras*$^{-/-}$) experiments, performed under similar conditions and histograms represent the mean ± SEM of the optical density of the bands, expressed as percentage over basal values (WT fibroblasts in 0.5% FCS, 100%); bands correspond to the ratio PCNA/total Erk expression (used as loading control). Statistically significant differences: &($p < 0.01$) vs. WT fibroblasts 48 h depleted; *($p < 0.05$) or **($p < 0.01$) vs. WT fibroblasts in basal conditions; #($p < 0.01$) or ##($p < 0.05$) vs. WT fibroblasts treated with 1 ng/mL TGF-β1; @($p < 0.05$) or @@($p < 0.01$) vs. N-*ras*$^{-/-}$ fibroblasts in basal conditions; $($p < 0.01$) vs. N-*ras*$^{-/-}$ fibroblasts treated with 1 ng/mL TGF-β1.

0.1 N NaOH. [^{3}H]-Proline incorporated into collagen proteins was measured in a β scintillation counter.

2.9. Wound-healing assay

In vitro scratched wounds were created with a straight incision on serum-starved confluent cell monolayers with a sterile disposable pipette tip. Cell migration into denuded area was monitored over a time course using digital microscopy and cell movement was calculated as the reduction of the wound area over time (in percentage, initial area of the wound: 100%).

2.10. Cell migration assay

Fibroblast migration was evaluated with a method based on the Boyden assay as previously described [32]. Cell suspension in 2% FCS medium was loaded into the chamber, and invading cells migrate through and attach to an 8 μm pore size polycarbonate membrane (bottom chamber containing 10% FCS medium), while non-invading cells remain above. The number of cells in the bottom of the chamber (migrating cells) was determined by the crystal violet method.

2.11. Cell transfection

N-Ras expression in N-*ras*$^{-/-}$ fibroblasts was induced by transfection of the pcEFL NRAS plasmid encoding N-Ras [40]. Fibroblasts were transfected for 20 h using JetPEI transfection reagent according to the manufacturer's instructions. Then, the cells were grown in 0.5% FCS DMEM medium for 24 h and cells were lysed for Western blot analysis.

2.12. Statistical methods

Data are expressed as mean ± standard error of the mean (SEM). The Kolmogorov–Smirnov test was used to assess the normality of the data distribution. Comparison of means was performed by two way analysis of variance (ANOVA) and Bonferroni post-test. Statistical differences between groups were assessed by the Student "t" test. Statistical analysis was performed using Graph Pad Prism version 5.00 for Windows, Graph Pad Software, San Diego California USA, www.graphpad.com. A "p" value lower than 0.05 was considered statistically significant.

3. Results

3.1. Activation of Ras and expression of Ras effectors, Erk and Akt

Total Ras expression levels, analyzed by Western blot, were slightly decreased in N-*ras*$^{-/-}$ with respect to WT fibroblasts (data not shown). To determine the effect of the absence of the N-Ras isoform on Ras activation, we analyzed cellular extracts from WT and N-*ras*$^{-/-}$ fibroblasts in basal conditions and under TGF-β1 treatment with Ras activation ELISA assay Kit. Basal Ras activation was slightly increased in N-*ras*$^{-/-}$ with respect to WT fibroblasts. Treatment with 1 ng/mL TGF-β1 for 24 h did not increase significantly Ras activation in fibroblasts (Fig. 1A).

We also analyzed by Western blot possible changes in the activation of MEK/Erk and PI3K/Akt pathways. The ratio phospho-Erk/Erk and phospho-Akt/Akt was significantly higher in basal conditions in N-Ras KO fibroblasts than in WT fibroblasts. TGF-β1 treatment for 24 h increased these ratios in WT fibroblasts, but no effect was observed in N-*ras*$^{-/-}$ fibroblasts (Fig. 1B and C).

3.2. ECM proteins synthesis in fibroblasts

In order to evaluate the possible differences in the expression of ECM proteins in the absence of the N-Ras isoform, we analyzed by RT-PCR and Western blot the basal and TGF-β1-induced expression of fibronectin and collagen type I in both N-*ras*$^{-/-}$ and WT fibroblasts. We previously performed a collagenase assay to elucidate which bands correspond to collagen, and thus 180 and 90 kDa bands were identified and quantified in order to measure collagen type I expression [33]. We also evaluated the synthesis of total collagen proteins by measuring [^{3}H]-proline incorporation into collagen proteins. Dose and time for TGF-β1 treatment (1 ng/mL, 24 h) was based on previous studies [32,33].

In basal conditions, collagen type I mRNA and protein expression, as well as total collagen synthesis, were significantly higher in N-*ras*$^{-/-}$ fibroblasts than in WT fibroblasts (Fig. 2A, C and E). Fibronectin protein expression was similar in both WT and N-*ras*$^{-/-}$ fibroblasts, but fibronectin mRNA expression was higher in absence of N-Ras (Fig. 2B and D). TGF-β1 increased total collagen synthesis as well as collagen type I and fibronectin expression (Fig. 2A–D). However, in N-*ras*$^{-/-}$ fibroblasts TGF-β1 did not induce any significant increase in total collagen synthesis with respect to the same cells in basal conditions (Fig. 2E). On the other hand, transfection with a plasmid containing N-Ras-encoding DNA in N-Ras KO fibroblasts induced a decrease in the expression of ECM proteins collagen I and fibronectin (Fig. 2F).

To assess the putative role of MEK/Erk and PI3K/Akt pathways in the regulation of ECM proteins expression in the absence of the N-Ras isoform, we analyzed the effect of their inhibition on both basal and TGF-β1-induced fibronectin and collagen I expression in N-*ras*$^{-/-}$ and WT fibroblasts by co-incubating the cells with the MEK 1/2 inhibitor U0126 (20 μM) or with the PI3K inhibitor LY294002 (20 μM) for 24 h. Basal expression of both collagen I and fibronectin were significantly reduced after Erk inhibition in WT fibroblasts but this reduction was not statistically significant in N-*ras*$^{-/-}$ fibroblasts (Fig. 3A and C). The inhibition of Erk phosphorylation induced a significant reduction in TGF-β1-induced fibronectin expression in WT fibroblasts (Fig. 3C), but it did not modify TGF-β1-induced collagen I or fibronectin expression in fibroblasts lacking N-Ras (Fig. 3A and C). PI3K inhibition significantly reduced both basal and TGF-β1-induced expression of collagen type I in both WT and N-*ras*$^{-/-}$ fibroblasts (Fig. 3B), but it did not modify significantly neither basal nor TGF-β1-induced fibronectin expression in both types of fibroblasts (Fig. 3D). The effect of both inhibitors on Erk and Akt phosphorylation is shown in Fig. 3E and F.

3.3. Fibroblast proliferation

We evaluated the role of the N-Ras isoform in fibroblast proliferation analyzing a) the total number of cells by nuclear staining with crystal violet, b) expression of Ki67 – a protein expressed during G1, S, G2 and M cell cycle phases [41] – and c) expression of PCNA – a component of replication and DNA repairing machinery [42]. Fibroblasts proliferation during 24 and 48 h, measured as the total number of cells, was significantly lower in N-*ras*$^{-/-}$ than in WT fibroblasts (Fig. 4A); moreover, PCNA expression (Fig. 4E) and the number of Ki67-possitive cells (Fig. 5A) after 24 h were also lower in N-*ras*$^{-/-}$ than in WT fibroblasts.

We also determined the effect of TGF-β1 treatment on cell proliferation. TGF-β1 (1 ng/mL, 48 h) increased fibroblast proliferation in both N-*ras*$^{-/-}$ and WT fibroblasts, (Fig. 4A). However, TGF-β1 induced increases in Ki67 and PCNA expressions only in WT fibroblasts but not in N-*ras*$^{-/-}$ fibroblasts (Figs. 4D and 5A).

We analyzed the effect of MEK and PI3K inhibition in TGF-β1-induced fibroblast proliferation by co-incubation with the MEK 1/2 inhibitor U0126 (20 μM) or with the PI3K inhibitor LY294002 (20 μM) for 24 h. PI3K inhibition reduced basal and TGF-β1-induced fibroblast proliferation, as well as Ki67 expression in WT and KO cells, although PCNA expression was not reduced after PI3K inhibition in KO fibroblasts (Figs. 4C, F and 5C). MEK inhibition only inhibited PCNA expression in WT fibroblasts (Fig. 4E), whereas TGF-β1-induced Ki67 expression was also reduced in the presence of the MEK inhibitor in both WT and KO cells (Fig. 5B); MEK inhibition did not induce any change in either basal or TGF-β1 induced fibroblast proliferation (Fig. 4B).

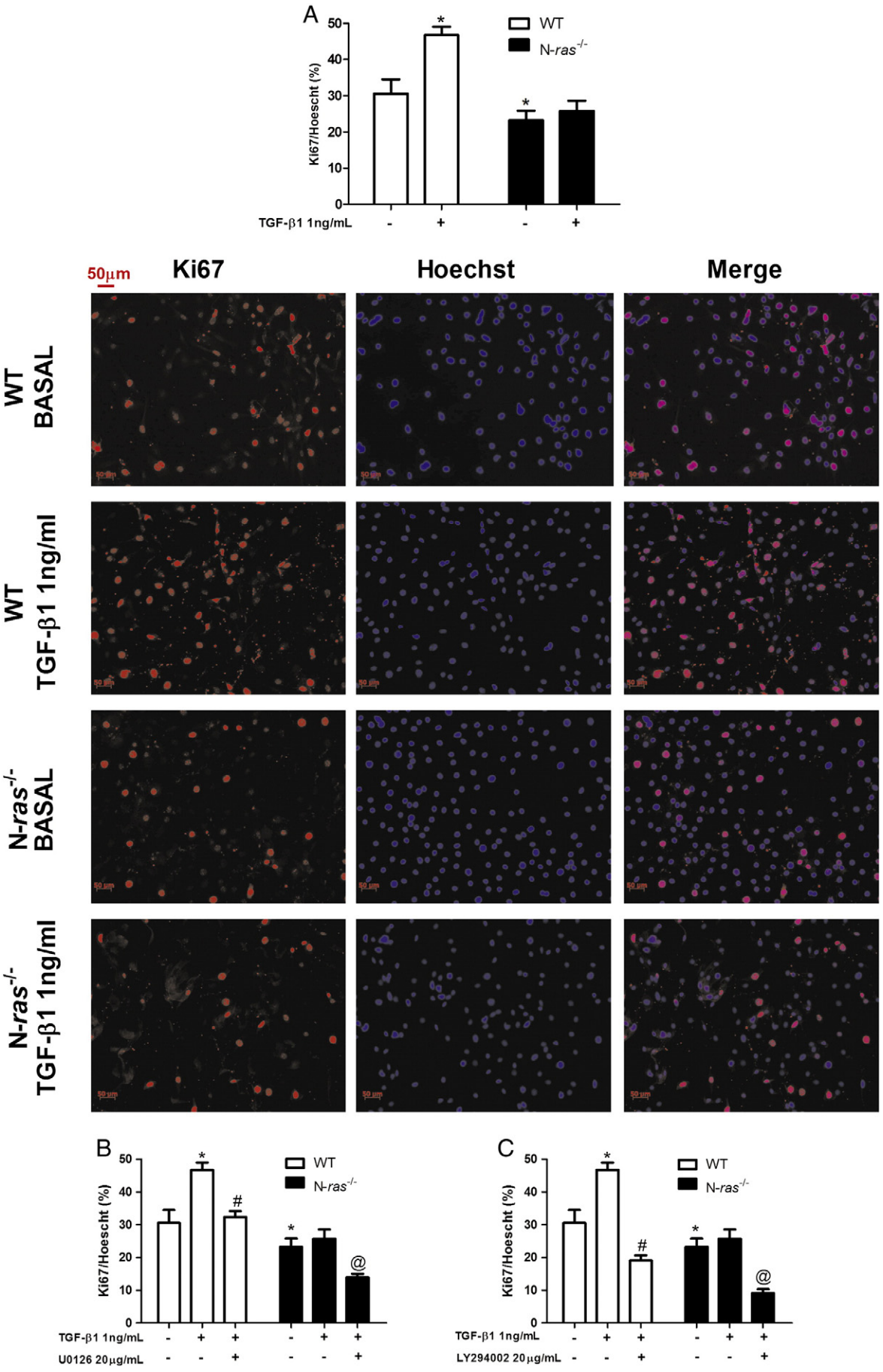
A
Ki67/Hoescht (%)
WT
N-ras-/-
TGF-β1 1ng/mL
50μm
Ki67
Hoechst
Merge
WT BASAL
WT TGF-β1 1ng/ml
N-ras-/- BASAL
N-ras-/- TGF-β1 1ng/ml
B
TGF-β1 1ng/mL
U0126 20μg/mL
C
TGF-β1 1ng/mL
LY294002 20μg/mL

3.4. Cell migration

Fibroblast migration was analyzed measuring the reduction in the wound area for 20 h in an in vitro wound-healing assay and by determining cell migration by use of a Boyden chamber. Time-course studies of wound closure area showed that cell movement in N-*ras*$^{-/-}$ fibroblasts was notably slower than in WT cells (Fig. 6A and B); moreover, fibroblast migration in Boyden chamber was also markedly decreased in N-*ras*$^{-/-}$ fibroblasts with respect to WT fibroblasts (Fig. 6E). Therefore, cell movement seems to be significantly restricted in fibroblasts lacking N-Ras.

Erk inhibition did not modify wound closure time in a significant manner in either N-*ras*$^{-/-}$ or WT fibroblasts (Fig. 6C), but decreased the number of migrating cells through the Boyden chamber in N-*ras*$^{-/-}$ fibroblasts (Fig. 6E). Akt inhibition increased wound closure times in WT fibroblasts to values similar to those of N-*ras*$^{-/-}$ fibroblasts (Fig. 6D) and reduced cellular migration through the Boyden chamber in both N-*ras*$^{-/-}$ and WT fibroblasts (Fig. 6E).

3.5. Effect of N-Ras knock-down in a different fibroblast cell clone

We performed additional experiments with a second N-Ras KO cell clone of immortalized fibroblasts. Supplementary Fig. 1 shows that the effect of the absence of N-Ras on fibroblast proliferation and in the expression of extracellular matrix proteins is similar to that observed in the previous studied clone. All these data seem to confirm that the effects observed in the absence of N-Ras are not due to the selection of a particular clone.

4. Discussion

Ras GTPase family members are crucial players in a variety of processes as cell proliferation, migration, or cytoskeletal changes [43,44]. Although there are several papers describing the relationships between Ras proteins and their effectors Erk and Akt, and in vivo renal fibrosis, including some from our group [45,46], this is the first study assessing the involvement of the N-Ras isoform and some intracellular pathways (MEK/Erk and PI3K/Akt) in fibroblast function and fibrosis development.

Loss of the ECM homeostasis is one of the main features of the fibrotic processes [47,48] and fibroblasts play a major role in fibrosis [30]. We observed a higher accumulation of one of the main ECM protein (collagen) in cultured fibroblasts without the N-Ras isoform than in WT fibroblasts, suggesting a possible modulator role of N-Ras in this process. Moreover, transfection with a plasmid containing N-Ras-encoding DNA in N-Ras KO fibroblasts decreased the expression of collagen I and fibronectin. It has been reported that N-Ras activation decreased mRNA expression of collagen type I genes in rat fibroblasts [49] and fibronectin accumulation in a human fibrosarcoma cell line [50–53]. We suggest that in unstimulated fibroblasts N-Ras probably acts either as a negative regulator of genes transcription pathways or as an activator of degrading enzymes for fibronectin and collagen type I, although the regulation of TGF-β1-induced collagen I and fibronectin expression seems to be N-Ras independent. Fibronectin expression is similar either in the presence or absence of N-Ras. However, our group has previously observed a decrease in fibronectin expression in fibroblasts lacking both H- and N-Ras [33], which suggests that fibronectin expression in basal conditions appears to be H-Ras dependent and independent of the presence of N-Ras.

The higher ECM accumulation observed in N-Ras KO fibroblasts may be related with the higher activation of phospho-Erk and phospho-Akt detected in those fibroblasts in basal conditions. Inhibition of Erk activation reduced collagen I and fibronectin expression in WT but not in N-*ras*$^{-/-}$ fibroblasts and did not induce significant changes in TGF-β1-induced collagen and fibronectin expression, suggesting that Erk activation is involved in ECM accumulation in basal conditions although the N-Ras isoform may be modulating collagen I and fibronectin expression through Erk-independent pathways. Although N-Ras KO fibroblasts show a higher phospho-Erk expression in basal conditions than WT fibroblasts, we have previously observed that H-Ras KO fibroblasts show no changes in phospho-Erk expression [32] and on the other hand, H- and N-Ras double KO fibroblasts exhibit significantly lower phospho-Erk levels than their WT controls [33], thus suggesting that phospho-Erk basal expression is differently regulated by each of the Ras isoforms. On the other hand, the implication of the PI3K/Akt pathway in ECM synthesis regulation is widely described in many cell lines [54–57] and in in vitro models of renal tubule-interstitial fibrosis [45]. Our data in WT and N-*ras*$^{-/-}$ fibroblasts agree with these studies and suggest that phospho-Akt expression is, at least partially, dependent of N-Ras isoform, which may down-regulate ECM accumulation through inhibition of Akt activation. These findings are in concordance with our previous studies showing that both N- and H-Ras isoforms may prevent the excessive ECM synthesis through down-regulation of PI3K/Akt activity in fibroblasts [32,33].

Fibroblast proliferation and migration are key processes in the development of renal fibrosis [30,31]. We observed that N-*ras*$^{-/-}$ fibroblasts showed less PCNA and Ki67 protein expressions and less proliferation than WT fibroblasts after 24 h in basal conditions. Reduced fibroblast proliferation may be related with the higher ECM production observed in N-*ras*$^{-/-}$ fibroblasts, as it was previously described by Weber and cols. in a tumoral pancreatic cell line [58]. It has been reported that TGF-β stimulates proliferation of fibroblasts [59–63]. Our results suggest that this proliferative effect induced by TGF-β is independent of N-Ras. In an in vivo study, early fibrotic changes induced by unilateral ureteral ligation were similar in N-*ras*$^{-/-}$ and in WT mice [64]. It should be noted that in early fibrotic changes after unilateral ureteral ligation, the participation of renal myofibroblasts is very limited [64]. Activation of Erk and Akt pathways may up- or down-regulate proliferation in many cell lines and in vitro models depending of the cell state and the signal duration. Generally, Erk activation increases proliferation [65–67]. However in proliferating cells, a high activation of the Erk pathway may induce cell cycle stop, senescence, apoptosis and differentiation, but a sustained and low activation of the Erk pathway is a normal feature of numerous proliferating systems [68–71]. PI3K activation also induces proliferation in renal fibroblasts [57], in NIH3T3 fibroblast treated with Wnt3a protein [72] and in lung fibroblast stimulated with ionic radiation [73]. In our study, fibroblast proliferation is inhibited by LY294002 in both WT and N-*ras*$^{-/-}$ fibroblasts and Erk inhibition reverts TGF-β1-induced-proliferation only in WT fibroblasts, although TGF-β1-induced PCNA expression did not change in N-*ras*$^{-/-}$ fibroblasts after Erk or Akt inhibition. Basal phospho-Erk levels are elevated in the absence of N-Ras, and these elevated levels may explain that the phospho-Erk inhibitor U0126 is not capable of reducing phospho-Erk levels low enough to affect the rate of cell proliferation. However, it is striking that phospho-Erk, a intracellular mediator usually involved in signaling pathways associated with stimulation of proliferation, is elevated in N-Ras KO fibroblasts, and these cells present a less proliferation in response to TGF-β1. This fact seems to suggest that TGF-β1-induced proliferation appears not to be phospho-Erk dependent in this cell type. On the other hand, previous studies from our group showed that TGF-β1-

Fig. 5. Ki67 expression in WT and N-*ras*$^{-/-}$ fibroblasts. Effect of TGF-β1 treatment (1 ng/mL) (A), phospho-Erk inhibition with 20 μM U0126 (B) and phospho-Akt inhibition with 20 μM LY294002 (C) on Ki67 expression evaluated by inmmunofluorescence. Lower panels in A show representative microphotographs (100×) of Ki67 immunostaining of different experiments, performed under similar conditions. Histograms represent the mean ± SEM of 33 (WT)-11 (N-*ras*$^{-/-}$) different fields analyzed, expressed as percentage of Ki67 stained cells (red)/Hoechst stained cells (blue). Statistically significant differences: *($p < 0.05$) or **($p < 0.01$) vs. WT fibroblasts in basal conditions; #($p < 0.01$) or ##($p < 0.05$) vs. WT fibroblasts treated with 1 ng/mL TGF-β1; @($p < 0.05$) or @@($p < 0.01$) vs. N-*ras*$^{-/-}$ fibroblasts in basal conditions; $($p < 0.01$) vs. N-*ras*$^{-/-}$ fibroblasts treated with 1 ng/mL TGF-β1.

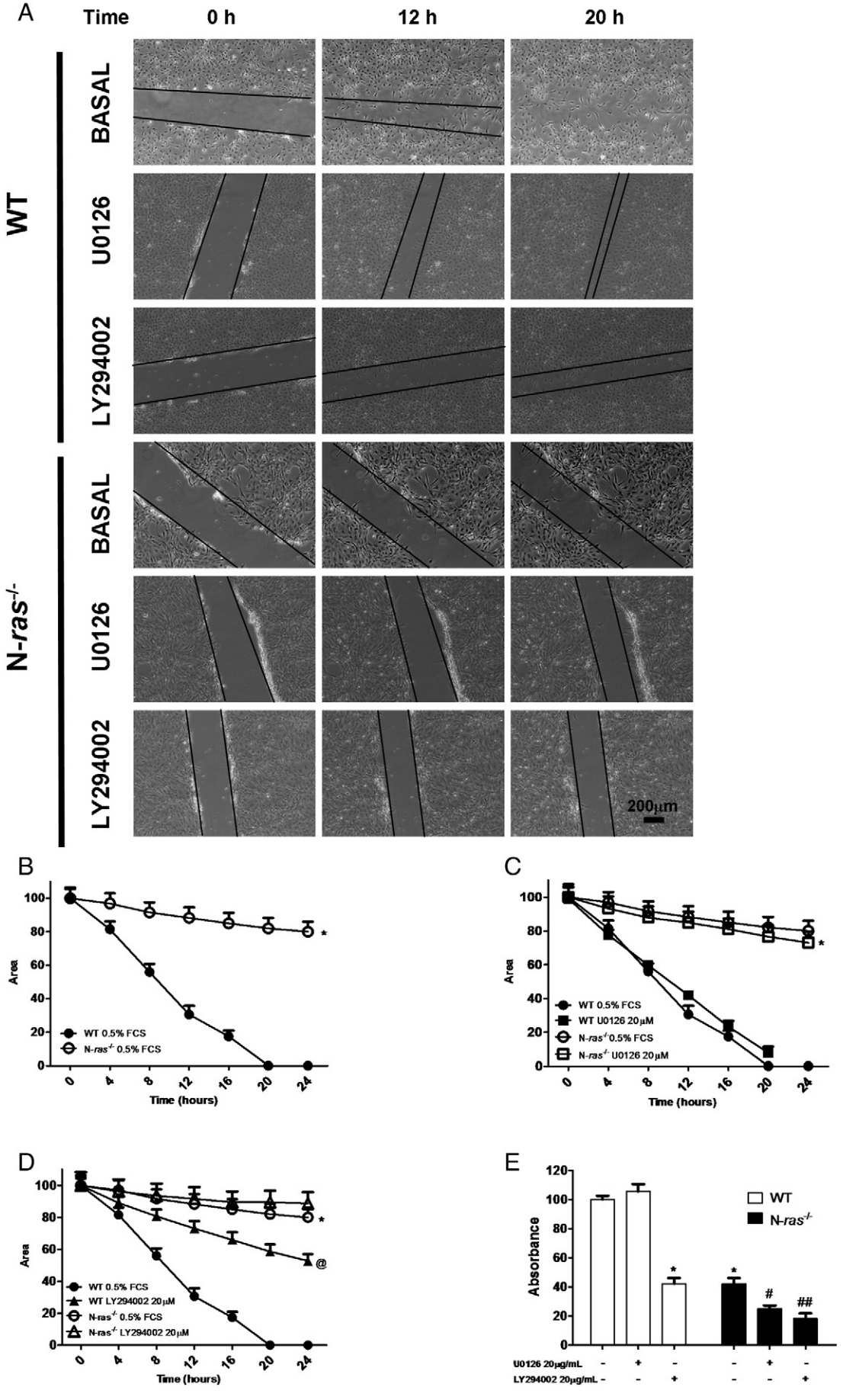
A
Time
0 h
12 h
20 h
WT
BASAL
U0126
LY294002
N-ras-/-
BASAL
U0126
LY294002
200μm
B
Area
Time (hours)
WT 0.5% FCS
N-ras-/- 0.5% FCS
C
Area
Time (hours)
WT 0.5% FCS
WT U0126 20μM
N-ras-/- 0.5% FCS
N-ras-/- U0126 20μM
D
Area
Time (hours)
WT 0.5% FCS
WT LY294002 20μM
N-ras-/- 0.5% FCS
N-ras-/- LY294002 20μM
E
Absorbance
WT
N-ras-/-
U0126 20μg/mL
LY294002 20μg/mL

induced expression of PCNA is lower in H- and N- double KO fibroblasts than in WT [29], which seems to confirm that the proliferative processes are mostly H-Ras dependent. Thus, most of our data suggest that Akt-mediated proliferation is independent of the presence of N-Ras, but N-Ras might modulate TGF-β1 induced-proliferation through phospho-Erk expression. The discrepancy found between the increased number of viable cells and PCNA and Ki67 expressions in response to TGF-β1 treatment may be due to the effect of N-Ras deficiency, but further experiments are needed to identify other proliferation-related intracellular pathways that are offsetting this effect.

We also show that N-Ras modulates fibroblast mobility. Previously, Fotiadou et al. [34] described a different modulating role of N-Ras and K-Ras proteins in fibroblast migration, showing that fibroblasts lacking N-Ras or K-Ras do not drive a correct cell migration and suggesting that N-Ras is more related with adhesion pathways. Our results confirm these data because N-Ras KO fibroblasts required more time to complete in vitro healing and to migrate through Boyden chambers. On the other hand, Akt inhibition (but not Erk inhibition) reduced migration in WT cells, suggesting the mediation of the PI3K/Akt pathway in fibroblast migration. In N-*ras*$^{-/-}$ fibroblasts the inhibition of Akt or Erk do not have any effect in postscratching closure-time, probably due to the lower migration rate of these cells in basal conditions, and also due to the fact that both cell proliferation and migration are involved in the closure time in cell wound assay. Nevertheless, Akt inhibition reduced the number of migrating cells through the Boyden chamber in both WT and N-*ras*$^{-/-}$ fibroblasts, but Erk inhibition only decreased the number of migrating N-*ras*$^{-/-}$ fibroblasts. These results evidence the involvement of Akt (and to a lesser extent, Erk) pathways in the regulation of fibroblast migration, although their relation with N-Ras are not sufficiently enlightened in this experimental model.

In conclusion, we described a modulator role of the N-Ras isoform in three of the main fibrotic processes in fibroblasts: ECM synthesis, proliferation and migration. In resting conditions, fibroblasts lacking N-Ras synthesize larger amounts of ECM and show reduced motility and reduced proliferative rate with a higher activation of Akt and Erk than WT fibroblasts. Our data suggest that in unstimulated cells, N-Ras might down-regulate Akt activation, reduce ECM accumulation and maintain normal proliferation and migration rates. N-Ras also mediates TGF-β1-induced collagen I and fibronectin expression through Erk-independent pathways, although TGF-β1 induced proliferation seems to be independent of N-Ras but modulated by Erk and Akt. Further experiments are needed to identify the crosstalk between the different signaling pathways induced by the activation of every Ras isoform.

Supplementary data to this article can be found online at http://dx.doi.org/10.1016/j.bbamcr.2013.07.008.

Acknowledgements

This work was supported by grants from European Commission Research Directorates General (ERG-Mobility-11, #508782), Instituto de Salud Carlos III (PS09/01067, PS09/01979, Retic RD06/0016/013 RedinRen, Retic RD12/0036/0001, Retic RD12/0036/0033 and Retic RD12/0036/0033), Ministerio de Ciencia e Innovación (BFU-2004-00285/BFI, BFU2011-23807 and SAF2010-15881) and Junta de Castilla y León (SA001/C05; SA029A05; GRS167/A/07 and Excellence Group GR100). IFC was supported by Junta de Castilla y León and European Social Fund.

References

[1] M. Barbacid, Ras genes, Annu. Rev. Biochem. 56 (1987) 779–827.
[2] N. Dhanasekaran, E. Premkumar Reddy, Signaling by dual specificity kinases, Oncogene 17 (1998) 1447–1455.
[3] E. Kerkhoff, U.R. Rapp, Cell cycle targets of Ras/Raf signalling, Oncogene 17 (1998) 1457–1462.
[4] M. Barbacid, Ras oncogenes: their role in neoplasia, Eur. J. Clin. Investig. 20 (1990) 225–235.
[5] E. Santos, S.R. Tronick, S.A. Aaronson, S. Pulciani, M. Barbacid, T24 human bladder carcinoma oncogene is an activated form of the normal human homologue of BALB- and Harvey-MSV transforming genes, Nature 298 (1982) 343–347.
[6] J. Leon, I. Guerrero, A. Pellicer, Differential expression of the ras gene family in mice, Mol. Cell. Biol. 7 (1987) 1535–1540.
[7] M.E. Furth, T.H. Aldrich, C. Cordon-Cardo, Expression of ras proto-oncogene proteins in normal human tissues, Oncogene 1 (1987) 47–58.
[8] I.A. Prior, J.F. Hancock, Compartmentalization of Ras proteins, J. Cell Sci. 114 (2001) 1603–1608.
[9] J.F. Hancock, K. Cadwallader, H. Paterson, C.J. Marshall, A CAAX or a CAAL motif and a second signal are sufficient for plasma membrane targeting of ras proteins, EMBO J. 10 (1991) 4033–4039.
[10] S. Roy, R. Luetterforst, A. Harding, A. Apolloni, M. Etheridge, E. Stang, B. Rolls, J.F. Hancock, R.G. Parton, Dominant-negative caveolin inhibits H-Ras function by disrupting cholesterol-rich plasma membrane domains, Nat. Cell Biol. 1 (1999) 98–105.
[11] S. Roy, S. Plowman, B. Rotblat, I.A. Prior, C. Muncke, S. Grainger, R.G. Parton, Y.I. Henis, Y. Kloog, J.F. Hancock, Individual palmitoyl residues serve distinct roles in H-ras trafficking, microlocalization, and signaling, Mol. Cell. Biol. 25 (2005) 6722–6733.
[12] E. Castellano, E. Santos, Functional specificity of ras isoforms: so similar but so different, Genes Cancer 2 (2011) 216–231.
[13] F. Calvo, L. Agudo-Ibanez, P. Crespo, The Ras-ERK pathway: understanding site-specific signaling provides hope of new anti-tumor therapies, Bioessays 32 (2010) 412–421.
[14] I. Arozarena, F. Calvo, P. Crespo, Ras, an actor on many stages: posttranslational modifications, localization, and site-specified events, Genes Cancer 2 (2011) 182–194.
[15] Y. Takai, T. Sasaki, T. Matozaki, Small GTP-binding proteins, Physiol. Rev. 81 (2001) 153–208.
[16] C. Wellbrock, M. Karasarides, R. Marais, The RAF proteins take centre stage, Nat. Rev. 5 (2004) 875–885.
[17] L.C. Cantley, The phosphoinositide 3-kinase pathway, Science (New York, N.Y.) 296 (2002) 1655–1657.
[18] G.C. Blobe, W.P. Schiemann, H.F. Lodish, Role of transforming growth factor beta in human disease, N. Engl. J. Med. 342 (2000) 1350–1358.
[19] M.H. Branton, J.B. Kopp, TGF-beta and fibrosis, Microbes Infect. 1 (1999) 1349–1365.
[20] R.A. Alcock, S. Dey, D. Chendil, M.S. Inayat, M. Mohiuddin, G. Hartman, L.K. Chatfield, V.S. Gallicchio, M.M. Ahmed, Farnesyltransferase inhibitor (L-744,832) restores TGF-beta type II receptor expression and enhances radiation sensitivity in K-ras mutant pancreatic cancer cell line MIA PaCa-2, Oncogene 21 (2002) 7883–7890.
[21] M. Iglesias, P. Frontelo, C. Gamallo, M. Quintanilla, Blockade of Smad4 in transformed keratinocytes containing a Ras oncogene leads to hyperactivation of the Ras-dependent Erk signalling pathway associated with progression to undifferentiated carcinomas, Oncogene 19 (2000) 4134–4145.
[22] M. Kretzschmar, J. Doody, I. Timokhina, J. Massague, A mechanism of repression of TGFbeta/Smad signaling by oncogenic Ras, Genes Dev. 13 (1999) 804–816.
[23] U. Haberstroh, G. Zahner, M. Disser, F. Thaiss, G. Wolf, R.A. Stahl, TGF-beta stimulates rat mesangial cell proliferation in culture: role of PDGF beta-receptor expression, Am. J. Physiol. 264 (1993) F199–F205.
[24] K. Matsuzaki, Modulation of TGF-beta signaling during progression of chronic liver diseases, Front. Biosci. 14 (2009) 2923–2934.
[25] J. Colicelli, Human RAS superfamily proteins and related GTPases, Sci. STKE 2004 (2004) RE13.
[26] J. Downward, Targeting RAS signalling pathways in cancer therapy, Nat. Rev. Cancer 3 (2003) 11–22.
[27] A. Rojas, M. Padidam, D. Cress, W.M. Grady, TGF-beta receptor levels regulate the specificity of signaling pathway activation and biological effects of TGF-beta, Biochim. Biophys. Acta 1793 (2009) 1165–1173.
[28] E. Castellano, J. Downward, RAS interaction with PI3K: more than just another effector pathway, Genes Cancer 2 (2011) 261–274.
[29] E. Castellano, J. Downward, Role of RAS in the regulation of PI 3-kinase, Curr. Top. Microbiol. Immunol. 346 (2010) 143–169.
[30] M.T. Grande, J.M. Lopez-Novoa, Fibroblast activation and myofibroblast generation in obstructive nephropathy, Nat. Rev. Nephrol. 5 (2009) 319–328.
[31] N. Hutchison, C. Fligny, J.S. Duffield, Resident mesenchymal cells and fibrosis, Biochim. Biophys. Acta 1832 (2013) 962–971.
[32] I. Fuentes-Calvo, A.M. Blazquez-Medela, N. Eleno, E. Santos, J.M. Lopez-Novoa, C. Martinez-Salgado, H-Ras isoform modulates extracellular matrix synthesis, proliferation, and migration in fibroblasts, Am. J. Physiol. 302 (2011) C686–C697.

Fig. 6. WT and N-*ras*$^{-/-}$ fibroblast migration. Representative images (50×) of wound closure at 0, 12 and 20 h in basal conditions and after incubation with UO126 or LY294002 in WT and N-*ras*$^{-/-}$ fibroblasts (A). Analysis of wound closure area in WT and N-*ras*$^{-/-}$ fibroblasts in basal condition (B); effect of phospho-Erk inhibition with 20 μM U0126 (C) and effect of phospho-Akt inhibition with 20 μM LY294002 (D) on cell mobility evaluated by the analysis of wound closure area and by migration through trans-wells in a Boyden chamber (E). Curve graphs in B–D represent the mean ± SEM of 5 (WT)–11 (N-*ras*$^{-/-}$) experiments evaluating the reduction of the wound area (in percentage, initial area of the wound: 100%) over time. Histograms in E represent mean ± SEM of the absorbance of 14 (WT)–3 (N-*ras*$^{-/-}$) experiments quantifying the number of crystal violet stained cells that go through the migration chamber, expressed as percentage vs. WT under basal conditions. Statistically significant differences: *($p < 0.05$) or **($p < 0.01$) vs. WT fibroblasts; #($p < 0.01$) or ##($p < 0.05$) vs. N-*ras*$^{-/-}$ fibroblasts in basal conditions.

[33] C. Martinez-Salgado, I. Fuentes-Calvo, B. Garcia-Cenador, E. Santos, J.M. Lopez-Novoa, Involvement of H- and N-Ras isoforms in transforming growth factor-beta1-induced proliferation and in collagen and fibronectin synthesis, Exp. Cell Res. 312 (2006) 2093–2106.
[34] P.P. Fotiadou, C. Takahashi, H.N. Rajabi, M.E. Ewen, Wild-type NRas and KRas perform distinct functions during transformation, Mol. Cell. Biol. 27 (2007) 6742–6755.
[35] M.T. Grande, I. Fuentes-Calvo, M. Arevalo, F. Heredia, E. Santos, C. Martinez-Salgado, D. Rodriguez-Puyol, M.A. Nieto, J.M. Lopez-Novoa, Deletion of H-Ras decreases renal fibrosis and myofibroblast activation following ureteral obstruction in mice, Kidney Int. 77 (2010) 509–518.
[36] L.M. Esteban, C. Vicario-Abejon, P. Fernandez-Salguero, A. Fernandez-Medarde, N. Swaminathan, K. Yienger, E. Lopez, M. Malumbres, R. McKay, J.M. Ward, A. Pellicer, E. Santos, Targeted genomic disruption of H-ras and N-ras, individually or in combination, reveals the dispensability of both loci for mouse growth and development, Mol. Cell. Biol. 21 (2001) 1444–1452.
[37] A. Montero, A. Rodriguez-Barbero, J.M. Lopez-Novoa, A role for platelet-activating factor in endothelin-1-induced rat mesangial cell proliferation, Eur. J. Pharmacol. 243 (1993) 235–240.
[38] R.J. Bryant, P.M. Banks, D.P. O'Malley, Ki67 staining pattern as a diagnostic tool in the evaluation of lymphoproliferative disorders, Histopathology 48 (2006) 505–515.
[39] P. Cortes, B.L. Riser, K. Asano, A. Rodriguez-Barbero, R.G. Narins, J. Yee, Effects of oral antihyperglycemic agents on extracellular matrix synthesis by mesangial cells, Kidney Int. 54 (1998) 1985–1998.
[40] D. Matallanas, I. Arozarena, M.T. Berciano, D.S. Aaronson, A. Pellicer, M. Lafarga, P. Crespo, Differences on the inhibitory specificities of H-Ras, K-Ras, and N-Ras (N17) dominant negative mutants are related to their membrane microlocalization, J. Biol. Chem. 278 (2003) 4572–4581.
[41] J. Gerdes, H. Lemke, H. Baisch, H.H. Wacker, U. Schwab, H. Stein, Cell cycle analysis of a cell proliferation-associated human nuclear antigen defined by the monoclonal antibody Ki-67, J. Immunol. 133 (1984) 1710–1715.
[42] Z. Kelman, PCNA: structure, functions and interactions, Oncogene 14 (1997) 629–640.
[43] K. Rajalingam, R. Schreck, U.R. Rapp, S. Albert, Ras oncogenes and their downstream targets, Biochim. Biophys. Acta 1773 (2007) 1177–1195.
[44] E.C. Stites, K.S. Ravichandran, A systems perspective of ras signaling in cancer, Clin. Cancer Res. 15 (2009) 1510–1513.
[45] A.B. Rodriguez-Pena, M.T. Grande, N. Eleno, M. Arevalo, C. Guerrero, E. Santos, J.M. Lopez-Novoa, Activation of Erk1/2 and Akt following unilateral ureteral obstruction, Kidney Int. 74 (2008) 196–209.
[46] A.B. Rodriguez-Pena, E. Santos, M. Arevalo, J.M. Lopez-Novoa, Activation of small GTPase Ras and renal fibrosis, J. Nephrol. 18 (2005) 341–349.
[47] A.A. Eddy, Progression in chronic kidney disease, Adv. Chronic Kidney Dis. 12 (2005) 353–365.
[48] Y. Liu, Cellular and molecular mechanisms of renal fibrosis, Nat. Rev. Nephrol. 7 (2011) 684–696.
[49] J.L. Slack, M.I. Parker, V.R. Robinson, P. Bornstein, Regulation of collagen I gene expression by ras, Mol. Cell. Biol. 12 (1992) 4714–4723.
[50] A. Hall, C.J. Marshall, N.K. Spurr, R.A. Weiss, Identification of transforming gene in two human sarcoma cell lines as a new member of the ras gene family located on chromosome 1, Nature 303 (1983) 396–400.
[51] S. Rasheed, W.A. Nelson-Rees, E.M. Toth, P. Arnstein, M.B. Gardner, Characterization of a newly derived human sarcoma cell line (HT-1080), Cancer 33 (1974) 1027–1033.
[52] K.A. Brenner, S.A. Corbett, J.E. Schwarzbauer, Regulation of fibronectin matrix assembly by activated Ras in transformed cells, Oncogene 19 (2000) 3156–3163.
[53] L.A. Chandler, S. Bourgeois, Posttranscriptional down-regulation of fibronectin in N-ras-transformed cells, Cell Growth Differ. 2 (1991) 379–384.
[54] M. Ivarsson, A. McWhirter, T.K. Borg, K. Rubin, Type I collagen synthesis in cultured human fibroblasts: regulation by cell spreading, platelet-derived growth factor and interactions with collagen fibers, Matrix Biol. 16 (1998) 409–425.
[55] V.S. Reddy, R.E. Harskamp, M.W. van Ginkel, J. Calhoon, C.E. Baisden, I.S. Kim, A.J. Valente, B. Chandrasekar, Interleukin-18 stimulates fibronectin expression in primary human cardiac fibroblasts via PI3K-Akt-dependent NF-kappaB activation, J. Cell. Physiol. 215 (2008) 697–707.
[56] D.A. Ricupero, C.F. Poliks, D.C. Rishikof, K.A. Cuttle, P.P. Kuang, R.H. Goldstein, Phosphatidylinositol 3-kinase-dependent stabilization of alpha1(I) collagen mRNA in human lung fibroblasts, Am. J. Physiol. 281 (2001) C99–C105.
[57] C.E. Winbanks, L. Grimwood, A. Gasser, I.A. Darby, T.D. Hewitson, G.J. Becker, Role of the phosphatidylinositol 3-kinase and mTOR pathways in the regulation of renal fibroblast function and differentiation, Int. J. Biochem. Cell Biol. 39 (2007) 206–219.
[58] K.S. Weber, G. Ostermann, A. Zernecke, A. Schroder, L.B. Klickstein, C. Weber, Dual role of H-Ras in regulation of lymphocyte function antigen-1 activity by stromal cell-derived factor-1alpha: implications for leukocyte transmigration, Mol. Biol. Cell 12 (2001) 3074–3086.
[59] I.A. Cunliffe, R.C. Rees, I.G. Rennie, The effect of TGF-beta 1 and TGF-beta 2 on the proliferation of human Tenon's capsule fibroblasts in tissue culture, Acta Ophthalmol. Scand. 74 (1996) 31–35.
[60] E.P. Kay, M.S. Lee, G.J. Seong, Y.G. Lee, TGF-beta s stimulate cell proliferation via an autocrine production of FGF-2 in corneal stromal fibroblasts, Curr. Eye Res. 17 (1998) 286–293.
[61] E.P. Kay, H.K. Lee, K.S. Park, S.C. Lee, Indirect mitogenic effect of transforming growth factor-beta on cell proliferation of subconjunctival fibroblasts, Investig. Ophthalmol. Vis. Sci. 39 (1998) 481–486.
[62] H. Werner, C.T. Roberts Jr., The IGFI receptor gene: a molecular target for disrupted transcription factors, Genes Chromosomes Cancer 36 (2003) 113–120.
[63] M. Valluru, C.A. Staton, M.W. Reed, N.J. Brown, Transforming growth factor-beta and endoglin signaling orchestrate wound healing, Front. Physiol. 2 (2011) 89.
[64] M.T. Grande, M. Arevalo, A. Nunez, J.B. Cannata-Andia, E. Santos, J.M. Lopez-Novoa, Targeted genomic disruption of H-ras and N-ras has no effect on early renal changes after unilateral ureteral ligation, World J. Urol. 27 (2009) 787–797.
[65] T. Ishida, M. Haneda, S. Maeda, D. Koya, R. Kikkawa, Stretch-induced overproduction of fibronectin in mesangial cells is mediated by the activation of mitogen-activated protein kinase, Diabetes 48 (1999) 595–602.
[66] M.D. Jiang, S.M. Zheng, H. Xu, W.Z. Zeng, Y. Zhang, H.P. Sun, Y.X. Wang, J.P. Qin, X.L. Wu, An experimental study of extracellular signal-regulated kinase and its interventional treatments in hepatic fibrosis, Hepatobiliary Pancreat. Dis. Int. 7 (2008) 51–57.
[67] S. Matthiesen, A. Bahulayan, O. Holz, K. Racke, MAPK pathway mediates muscarinic receptor-induced human lung fibroblast proliferation, Life Sci. 80 (2007) 2259–2262.
[68] C. Kahan, K. Seuwen, S. Meloche, J. Pouyssegur, Coordinate, biphasic activation of p44 mitogen-activated protein kinase and S6 kinase by growth factors in hamster fibroblasts. Evidence for thrombin-induced signals different from phosphoinositide turnover and adenylylcyclase inhibition, J. Biol. Chem. 267 (1992) 13369–13375.
[69] K.M. Pumiglia, S.J. Decker, Cell cycle arrest mediated by the MEK/mitogen-activated protein kinase pathway, Proc. Natl. Acad. Sci. U. S. A. 94 (1997) 448–452.
[70] M.S. Qui, S.H. Green, PC12 cell neuronal differentiation is associated with prolonged p21ras activity and consequent prolonged ERK activity, Neuron 9 (1992) 705–717.
[71] K. Roovers, R.K. Assoian, Integrating the MAP kinase signal into the G1 phase cell cycle machinery, Bioessays 22 (2000) 818–826.
[72] S.E. Kim, W.J. Lee, K.Y. Choi, The PI3 kinase-Akt pathway mediates Wnt3a-induced proliferation, Cell. Signal. 19 (2007) 511–518.
[73] C.S. Kim, J.K. Kim, S.Y. Nam, K.H. Yang, M. Jeong, H.S. Kim, C.S. Kim, Y.W. Jin, J. Kim, Low-dose radiation stimulates the proliferation of normal human lung fibroblasts via a transient activation of Raf and Akt, Mol. Cells 24 (2007) 424–430.